Observation of Metal-Vacuum-Metal Tunneling, Field Emission, and the Transition Region

Russell Young, John Ward, and Fred Scire
National Bureau of Standards, Washington, D. C. 20234
(Received 26 August 1971)

We report what we believe are the first observations of metal-vacuum-metal tunneling. A field emitter is brought close to a metal surface and the current-voltage characteristic is measured in three regions: the Fowler-Nordheim region, the intermediate region, and-and the metal-vacuum-metal region.

Certain problems encountered in the investigation of thin-film tunnel devices[1] might be illuminated by studying the characteristics of vacuum-insulated tunnel diodes, which we designated as metal-vacuum-metal (MVM) diodes. In particular, the advantage of being able to (1) change electrode spacing conveniently, (2) eliminate the effects of insulator material, and (3) characterize carefully the two electrode surfaces, could be exploited in testing the present theoretical framework of tunneling. We report here what we believe are the first observations of MVM tunneling and the transition to field emission.

The instrument employed in this study is designed to measure the microtopography of a metal surface by scanning a field-emission point close to the metal surface.[2,3] The field emitter is mounted on a piezoelectric crystal which is part of a servo system designed to keep the emitter a constant distance of a few hundred angstroms above the surface. Two other piezo units scan the emitter in orthogonal directions parallel to the surface. The instrument, called the Topografiner, produces a high-resolution topographic map of the surface.

In present experiments, the servo loop and scanning piezos were disconnected and a carefully regulated adjustable voltage was applied to the altitude piezo in order to move the tungsten emitter very close to the platinum surface. The instrument is mounted on a low-vibration stand with a vertical period of 1 Hz and is surrounded by an acoustic shield. During the tunneling (MVM) experiments reported here the instrument was remotely operated to reduce acoustic noise further.

In all of the measurements, except Fig. 3, the field at the emitter surface was fixed by passing a constant current through the emitter. For a fixed emitter field, the emitter-to-surface voltage has been determined by solving Laplace's equation in prolate spheroidal coordinates.[4] By comparing this calculation with experimental curves for emitter-to-surface voltage versus distance it is possible to determine the emitter radius of curvature.[2] When the emitter-to-surface spacing is less than one tenth of the emitter radius of curvature, the voltage approaches a linear function of emitter-to-surface spacing (parallel-plate approximation), and the field at the surface of the emitter can be determined directly from emitter voltage versus distance. Figure 1 shows the emitter-to-surface voltage as a function of piezo voltage (distance) for a situation where the emitter has previously contacted the surface, resulting in flattening of the emitter apex. After annealing (cleaning), the flattened emitter produced a curve with a long linear region giving an excellent opportunity to determine the field strength at the surface of the emitter. The structure in the curves is due to the individual wires on the ten-turn potentiometer used to vary the piezo voltage. The field strength determined from Fig. 1 was 0.381 V/Å with an estimated accuracy of 5%.

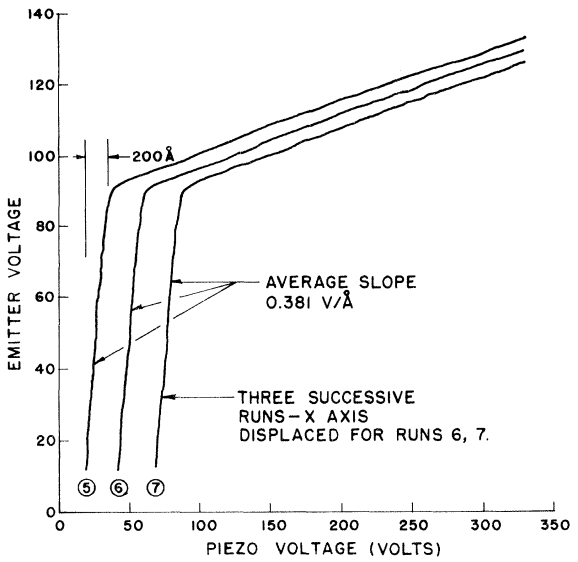

FIG. 1. Emitter-to-surface voltage versus piezo voltage. The piezo element, calibrated interferometrically, has a deflection factor of 13.0 Å/V. The slope of the straight-line portion of the left-hand side of the curves gives the field strength at the emitter surface directly.

Since the relationship between voltage and field strength was known, it was then possible to measure emission current versus applied field and to make a Fowler-Nordheim plot in terms of the field. We neglect the small change in average work function with spacing.

The Fowler-Nordheim (F-N) equation can be written in the following logarithmic form[5]:

$$\log\frac{i}{F^2}=\log\left(1.54\times10^{-6}\frac{A_0}{\varphi_0{}^2t^2(y)}\right)-\left[6.83\times10^{7}\frac{\varphi_0{}^{3/2}}{F}v(y)\right], \tag{1}$$

where F is the field strength in volts per centimeter, i is the field-emission current density in amperes per square centimeter, A_0 is the effective emitting area in square centimeters, φ_0 is the emitter work function in electron volts, and $v(y)$ and $t(y)$ are slowly varying elliptic functions. The intercept of the F-N plot is the first term on the right-hand side of Eq. (1). The slope is obtained by taking the derivative of Eq. (1) with respect to $1/F$ and is given by

$$m=-0.296\varphi_0{}^{3/2}s(y). \tag{2}$$

Application of Eqs. (1) and (2) to the F-N data yield the following values: $\varphi=4.60$ eV, $A_0=18.9\times10^{-10}$ cm^2. The techniques discussed above were used to determine the emitter radius (8100 Å) and the field strength used in the F-N plot (0.381 V/Å). The average work function at the apex of a tungsten emitter is somewhat higher than the overall average work function for tungsten due to the presence of the high-work-function (110) region at the apex. The value obtained is very reasonable. After accounting for the fact that the F-N data were taken when the 8100-Å emitter was only about 2000 Å above the surface, the effective emitting area has been found to be consistent with the emitter radius.[2] The details of the above analysis will be given in a forthcoming publication.[2] They have been summarized above to demonstrate that the F-N equation adequately describes the operation of the instrument when the emitter is located a few hundred angstroms above the surface and to establish the connection between field emission and MVM tunneling. Future experiments involving an extremely flat surface, a very smooth emitter of uniform work function, and further reduction in noise and vibration are expected to provide a critical test of the F-N equation.

Simmons has derived a general expression which describes the current density versus voltage over the full range from close-spaced MVM to field-emission tunneling.[6] The most general expression for current density, applicable to barriers which include the image potentials at both surfaces, is given by[6]

$$J=\frac{e}{2\pi h(\beta\Delta S)^2}\{\bar{\varphi}\exp(-A\bar{\varphi}^{1/2})-(\bar{\varphi}+eV)\exp[-A(\bar{\varphi}+eV)^{1/2}]\}, \tag{3}$$

where

$$A=\frac{4\pi\beta\Delta S\sqrt{(2m_e)}}{h},\quad \beta\simeq1,\quad \bar{\varphi}=\frac{1}{\Delta S}\int_{S_1}^{S_2}\varphi(X)\,dx,$$

$\varphi(x)$ is the potential energy of an electron between the two metal surfaces, S_1 and S_2 are the distances from the first surface to the place where the potential energy equals the Fermi energy near surfaces 1 and 2, respectively, $\Delta S=S_2-S_1$, m_e is the electron mass, and V is the potential between the two electrodes. For the low-voltage (MVM) range ($eV\ll\varphi_0$),

$$J=\frac{\sqrt{(2m_e)}}{\Delta S}\left(\frac{e}{h}\right)^2\bar{\varphi}^{1/2}V\exp(-A\bar{\varphi}^{1/2}) \tag{4}$$

which gives the expected linear dependence of current density on applied voltage.

Equations (3) and (4) predict an extremely strong dependence of J on electrode spacing. When measuring emission current versus spacing, unless electrode position control is extraordinarily good, it is experimentally advantageous to employ the constant-current mode of operation and measure interelectrode voltage versus spacing. We therefore plot in Fig. 2 the calculated voltage needed to maintain a constant emission current versus distance. Note the linear F-N region ($F=0.33$ V/Å), the sharp drop in potential in the transition region, and the extremely low-voltage MVM region. The dashed curve does not represent actual data, but rather depicts our experience, when decreasing the spacing, of being able to reduce the potential smoothly to about 8 V and then suddenly observing a precipitous drop in the potential to less than 1 V. This effect clearly has metrological applications in that it is possible to use this device as a noncontacting

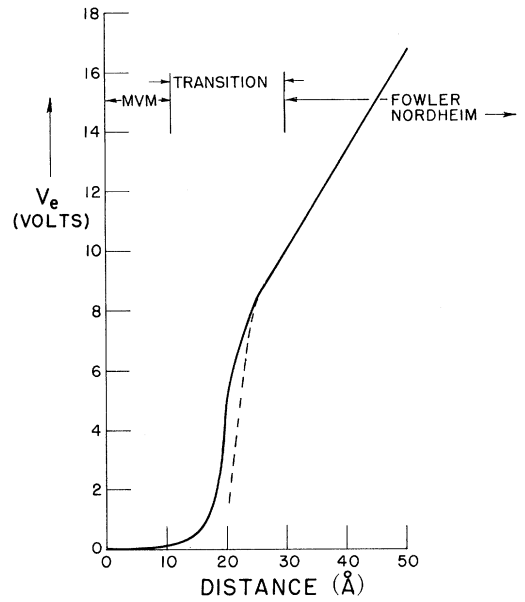

FIG. 2. Calculated tunnel voltage versus distance for a constant tunneling current density of 50 A/cm^2. The dotted line depicts our experience in attempting to measure this function. As the emitter approached the surface, the emitter voltage decreased smoothly along the F-N curve until $V_e = 8$ V, when V_e suddenly dropped precipitously to less than 1 V.

probe capable of determining the position of a metallic surface within perhaps 3 to 6 Å (one to two atom layers).

A second more quantitative measurement was made by biasing the elevation piezo so as to place the emitter within a few tens of angstroms of the surface and using an additional low-voltage power supply to move the emitter very close to the surface. The total piezo voltage was measured with a digital voltmeter with a precision of 0.1 V (~1.3 Å). Thus it was possible, during an extremely quiet period, to move the emitter by about 1-Å steps. Mechanical vibrations on the angstrom level were the limiting factor. After setting the spacing, the emitter-to-surface voltage was scanned over an appropriate voltage range, the current was measured with an electrometer, and the current-voltage characteristic was plotted with an X-Y recorder. The results are shown in Fig. 3. We have chosen three regions: the lower (closest) limit of the F-N regime, an intermediate spacing, and one near the upper limit of MVM regime. The gap values were determined from the current density and the F-N and MVM theories. The MVM tunneling resistivity $\sigma (= V/J)$ is approximately 4×10^{-3} Ω cm^2. The current-voltage characteristic is linear in the MVM region as expected.

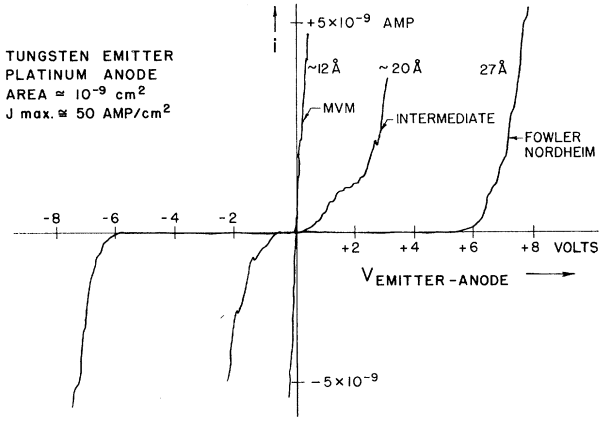

FIG. 3. Tunneling current versus voltage characteristic for three different emitter-to-surface spacings. Note the linear MVM characteristic.

A new instrument for MVM studies has been constructed and is now under test. The scanning system has been eliminated, resulting in a much more rugged device. Coarse adjustment is made with a helium-operated, thick-walled diaphragm so that the unit can be operated in a cryostat. In addition, further precautions against shaking and vibration will be needed before precision experiments can be performed. Such a device should have many applications. The effect of crystallographic orientation of the electrodes, with due attention to surface cleanliness, could be readily studied. Lambe and Jaklevic[7] have shown that inelastic tunneling can be used to study the vibrational spectra of molecules imbedded in an oxide matrix. MVM tunneling could be used to study the vibrational spectra of molecules, and perhaps atoms, adsorbed on clean, well characterized, single-crystal surfaces, possibly extending to the study of electronic excitation of adsorbed species. Other applications abound.

[1] *Tunneling Phenomena in Solids*, edited by E. Burstein and S. L. Lunqvist (Plenum, New York, 1969).
[2] R. Young, J. Ward, and F. Scire, to be published.
[3] R. Young, Rev. Sci. Instrum. 37, 275 (1966).
[4] A. M. Russell, J. Appl. Phys. 33, 970 (1962).
[5] R. H. Good and E. W. Müller, in *Handbuch der Physik*, edited by S. Flügge (Springer, Berlin, 1956), Vol. XXI.
[6] J. G. Simmons, J. Appl. Phys. 34, 1793 (1963).
[7] J. L. Lambe and R. C. Jaklevic, Phys. Rev. 165, 821 (1968).